The AMPK agonist AICAR inhibits the growth of EGFRvIII-expressing glioblastomas by inhibiting lipogenesis

Deliang Guo[a], Isabel J. Hildebrandt[b], Robert M. Prins[c], Horacio Soto[c], Mary M. Mazzotta[d], Julie Dang[a], Johannes Czernin[b,g], John Y.-J. Shyy[h], Andrew D. Watson[d], Michael Phelps[b,g,1], Caius G. Radu[b,g], Timothy F. Cloughesy[e,f], and Paul S. Mischel[a,b,f,g,1]

[a]Department of Pathology & Laboratory Medicine; [b]Department of Molecular & Medical Pharmacology; [c]Division of Neurosurgery, Department of Surgery; [d]Division of Cardiology, Department of Medicine; [e]Department of Neurology; [f]The Henry Singleton Brain Tumor Program and The Jonsson Comprehensive Cancer Center, The David Geffen UCLA School of Medicine, Los Angeles, CA 90095; [g]Institute for Molecular Medicine, University of California, Los Angeles, CA 90095; and [h]Division of Biomedical Sciences, University of California, Riverside, CA 92521.

Contributed by Michael Phelps, June 16, 2009 (sent for review February 24, 2009)

The EGFR/PI3K/Akt/mTOR signaling pathway is activated in many cancers including glioblastoma, yet mTOR inhibitors have largely failed to show efficacy in the clinic. Rapamycin promotes feedback activation of Akt in some patients, potentially underlying clinical resistance and raising the need for alternative approaches to block mTOR signaling. AMPK is a metabolic checkpoint that integrates growth factor signaling with cellular metabolism, in part by negatively regulating mTOR. We used pharmacological and genetic approaches to determine whether AMPK activation could block glioblastoma growth and cellular metabolism, and we examined the contribution of EGFR signaling in determining response in vitro and in vivo. The AMPK-agonist AICAR, and activated AMPK adenovirus, inhibited mTOR signaling and blocked the growth of glioblastoma cells expressing the activated EGFR mutant, EGFRvIII. Across a spectrum of EGFR-activated cancer cell lines, AICAR was more effective than rapamycin at blocking tumor cell proliferation, despite less efficient inhibition of mTORC1 signaling. Unexpectedly, addition of the metabolic products of cholesterol and fatty acid synthesis rescued the growth inhibitory effect of AICAR, whereas inhibition of these lipogenic enzymes mimicked AMPK activation, thus demonstrating that AMPK blocked tumor cell proliferation primarily through inhibition of cholesterol and fatty acid synthesis. Most importantly, AICAR treatment in mice significantly inhibited the growth and glycolysis (as measured by ^{18}fluoro-2-deoxyglucose microPET) of glioblastoma xenografts engineered to express EGFRvIII, but not their parental counterparts. These results suggest a mechanism by which AICAR inhibits the proliferation of EGFRvIII expressing glioblastomas and point toward a potential therapeutic strategy for targeting EGFR-activated cancers.

To mediate cell growth and proliferation, mTOR acts through the canonical PI3K pathway via 2 distinct complexes, mTORC1 and mTORC2. mTORC1 uniquely integrates growth factor signaling through S6K1 with cellular metabolism underscoring its value as a cancer target (1–3). mTOR signaling through S6K1 has recently been identified as a critical step in glial transformation (4), and it has been demonstrated to be greatly elevated in patients with mutant EGFR (5). Further, recent work suggests that persistent mTOR/S6K1 signaling may underlie clinical resistance to EGFR inhibitors (6). Thus, strategies for effectively inhibiting mTORC1 are needed.

In glioblastoma, attempts to target mTOR with rapamycin and its analogues have largely failed to show efficacy (7–9), mediated by difficulty in fully inhibiting mTORC1 signaling and by emergence of a feedback loop, that activates pro-growth, pro-survival Akt signaling (10). Rapamycin analogues also activate MAPK through a PI3K-dependent mechanism in other cancer types, suggesting additional potential mechanisms of clinical resistance and raising the need for alternative strategies to target mTOR signaling in patients (11).

AMPK is a metabolic checkpoint downstream of the LKB1 tumor suppressor that integrates growth factor receptor signaling with cellular energy status. AMPK inhibits mTORC1 by activating the tuberous sclerosis complex 2 and by direct inhibitory phosphorylation of the mTOR binding partner raptor to limit cellular proliferation (12–14). Therefore, activation of AMPK could potentially be a strategic target, particularly in EGFR-driven cancers that have high levels of mTOR/S6K1 activity. We set out to determine whether AMPK activation could inhibit the growth of glioblastoma and other EGFR-activated cancers.

Results

The AMPK Agonist AICAR Is More Effective than Rapamycin in Blocking the Growth of EGFR-activated Glioblastoma Cells. We have previously shown that feedback activation of Akt signaling significantly inhibits the clinical efficacy of rapamycin (10). This appears to be mediated through S6K1 inhibition and up-regulation of receptor tyrosine kinases or their substrates (11, 15), although the factors that mediate feedback activation in patients have yet to be fully elucidated. Here we asked whether expression of the most common EGFR mutant, constitutively active, ligand-independent mutant EGFRvIII (16, 17) could accentuate the feedback activation of Akt in response to rapamycin. In U87 glioblastoma cells transfected to express the EGFRvIII mutant, 1 nM rapamycin fully inhibited S6K phosphorylation and induced significant Akt phosphorylation. In contrast, no feedback activation of Akt was detected in parental U87 cells, despite complete inhibition of S6K Thr-389 phosphorylation (Fig. 1*A*).

To determine whether AMPK activation acted in a similar manner to rapamycin, U87, U87-EGFRvIII, and U87 cells transfected with wild-type EGFR were treated with the AMPK agonist AICAR. Unexpectedly, AICAR treatment up to 24 h did not induce Akt Ser-473 or Thr-308 phosphorylation in any of the cell lines despite inhibition of S6K1 and S6 phosphorylation (Fig. 1*B* and Fig. S1). Moreover, AICAR inhibited tumor growth with significantly enhanced efficacy in glioblastoma cells expressing

Author contributions: D.G., T.F.C., and P.S.M. designed research; D.G., I.J.H., R.M.P., H.S., M.M.M., and J.D. performed research; J.C., J.Y.-J.S., A.D.W., M.E.P., and C.G.R. contributed new reagents/analytic tools; D.G., I.J.H., R.M.P., J.C., J.Y.-J.S., A.D.W., M.E.P., C.G.R., T.F.C., and P.S.M. analyzed data; and D.G. and P.S.M. wrote the paper.

The authors declare no conflict of interest.

Freely available online through the PNAS open access option.

[1]To whom correspondence may be addressed. E-mail: pmischel@mednet.ucla.edu or mphelps@mednet.ucla.edu.

This article contains supporting information online at www.pnas.org/cgi/content/full/0906606106/DCSupplemental.

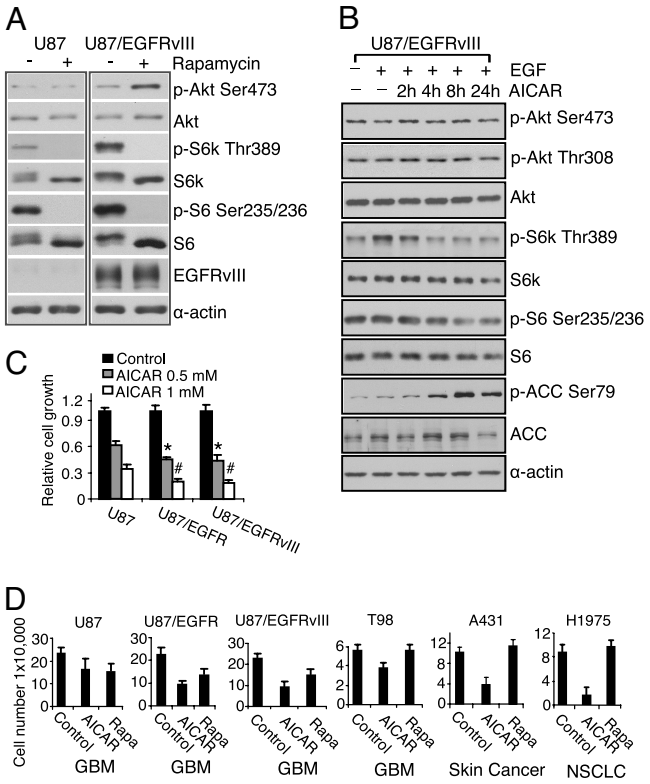

Fig. 1. AICAR inhibits the growth of EGFR-activated cancer cell lines, including glioblastoma cells. (*A*) Western blot analysis demonstrated Akt Ser-473 phosphorylation in U87-EGFRvIII, but not U87 cells in response to rapamycin (1 nM) for 24 h. (*B*) Immunoblot analysis of effect of AICAR (0.5 mM) on Akt and mTORC1 signaling. U87-EGFRvIII cells were treated for up to 24 h and effect on signaling pathways was determined at indicated time points. AICAR (0.5 mM) treatment for up to 24 h inhibited mTOR signaling (S6K and S6 phosphorylation), but does not induce Akt phosphorylation. AICAR also phosphorylated AMPK downstream target gene ACC. (*C*) U87, U87-EGFRvIII, and U87-EGFR glioblastoma cells were seeded in 96-well plates for 24 h and then treated for 3 days with AICAR at the doses indicated. Relative growth was measured using the WST assay (Chemicon). AICAR was significantly more effective at blocking the growth of wild-type EGFR or EGFRvIII- expressing glioblastoma cells, relative to their parental U87 counterparts (*, $P < 0.05$; #, $P < 0.05$). (*D*) AICAR (0.5 mM) was more effective than rapamycin (Rapa 1 nM) in blocking the growth of cancer cells with activated EGFR signaling. Cell lines were treated with indicated drugs for 3 days, and cell number was determined by trypan exclusion. EGFR level of cell line is U87 (low expression), U87/EGFR (high expression), U87/EGFRvIII (high expression/mutation), T98 (high expression), A431 (amplification), and H1975 (L858R1/T790M mutation); cancer cell line type is indicated below the graph. Control cells were treated with ethanol, the diluent, alone (1:1,000).

wild-type EGFR or EGFRvIII ($P < 0.05$ for each) (Fig. 1*C*). Across a spectrum of cancer cells with activated EGFR (including EGFRvIII) expressing U87 glioblastoma cells, T98 glioblastoma cells, EGFR-amplified A431 cells, and H1975 non-small cell lung cancer cells with activating L858R/T790M EGFR mutation (18), AICAR was highly efficacious at blocking tumor cell growth even in cell lines that were relatively insensitive to the mTORC1 inhibitor rapamycin (Fig. 1*D*).

To confirm that the anti-growth effect of AICAR was mediated through AMPK, we transduced glioblastoma cells with a constitutively active AMPK adenovirus. This treatment mimicked the effect of AICAR and significantly inhibited the proliferation of EGFRvIII expressing U87 glioblatoma cells (Fig. 2*A*). Concordant with these findings, the AMPK specific inhibitor Compound C (19) and AMPKα1/α2 siRNA both suppressed AICAR's ability to promote AMPK Thr-172 and ACC Ser-79 phosphorylation and to inhibit

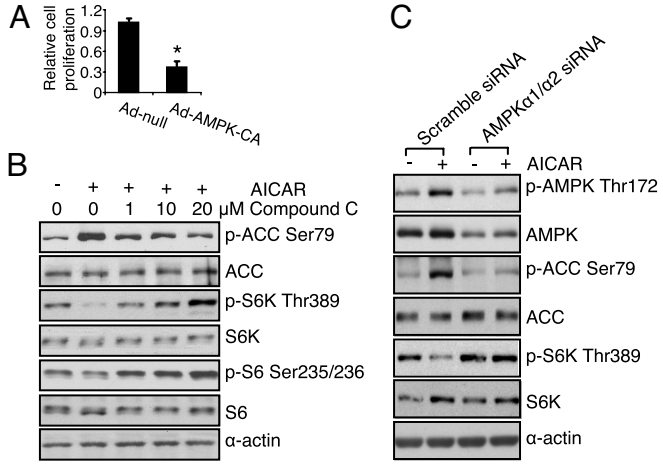

Fig. 2. The effect of AICAR on tumor growth and mTORC1 signaling is mediated through activation of AMPK. (*A*) Cells were infected by constitutively active AMPK adenovirus (Ad-AMPK-CA, 50 MOI) for 3 days, the growth of EGFRvIII expressing glioblastoma cells was inhibited by 65 ± 3.1%, *, $P < 0.001$ compared with cells infected by empty vector adenovirus (Ad-null, 50 MOI). (*B*) U87/EGFRvIII cells were treated with Compound C (1 μM, 10 μM, or 20 μM) for 30 min before AICAR (0.5 mM) treatment for 6 h. Cells were lysed and effect on signal transduction was determined by western blot using indicated antibodies. (*C*) U87/EGFRvIII cells were transfected with scrambled siRNA or AMPKα1/α2 siRNA (100 μM) for 48 h, then treated with AICAR (0.5 mM) for 6 h, followed by stimulation with EGF (20 ng/mL) for 15 min. Cellular lysates were the probed by western blot using indicated antibodies.

S6K Thr-389 phosphorylation (Fig. 2 *B* and *C*). These results indicate that AICAR's effects were mediated through activation of AMPK. We also treated tumor cells with 2, 4-dinitrophenol (DNP), which activates AMPK through an alternative mechanism (20). Like AICAR, DNP promoted AMPK Thr-172 phosphorylation and inhibited glioblastoma cell growth, with significantly enhanced efficacy in the EGFR and EGFRvIII-expressing glioblastoma cells ($P < 0.01$ for each) (Fig. S2), demonstrating that AMPK is a potent negative regulator of glioblastoma cell growth, particularly in EGFR-activated tumor cells.

The Inhibitory Effect of AICAR Is Not Fully Mediated by Inhibition of mTOR Signaling. Given the enhanced efficacy of AICAR relative to rapamycin in EGFR-activated tumor cells (Fig. 1*D*), and the fact that AMPK has multiple targets in addition to mTOR, we set out to determine whether other signaling pathways may contribute to response of these tumor cells to AICAR. To test whether AICAR's anti-growth effect was mediated by limiting mTORC1 signaling, we assessed the relative efficacy of AICAR and rapamycin to suppress the phosphorylation of downstream mTORC1 mediators, S6K and S6. As previously reported, rapamycin completely abolished S6K1 and S6 phosphorylation (at both the Ser-235/236 and Ser-240/244 sites) (Fig. 3*A*). In contrast, AICAR treatment resulted in substantially less inhibition of S6K1 and S6 phosphorylation than rapamycin treatment (Fig. 3*A*), despite its greater efficacy at blocking tumor cell proliferation (Fig. 3*C* and Fig. S3). These results suggested that the enhanced efficacy of AICAR was not mediated by more complete inhibition of mTORC1 signaling. To further test this possibility, we examined the effect of PTEN reconstitution on tumor cell sensitivity to AICAR and rapamycin. PTEN has been shown to limit sensitivity to rapamycin by inhibiting PI3K pathway activation and decreasing tumor cell dependence on mTORC1 signaling (21). Consistent with this model, PTEN add-back significantly inhibited the efficacy of rapamycin despite complete inhibition of S6K and S6 phosphorylation (Fig. 3 *B* and *C*). In contrast, AICAR demonstrated enhanced efficacy in PTEN-reconstituted tumor cells (Fig. 3*C*). Taken together, these data strongly suggest

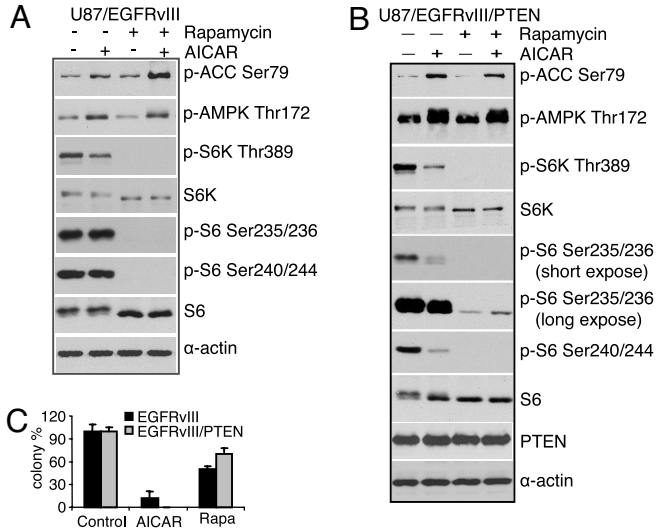

Fig. 3. The anti-growth effect of AICAR is only partially mediated through inhibition of mTOR signaling. (*A*) U87/EGFRvIII cells were treated by AICAR (0.5 mM) or rapamycin (1 nM) for 6 h, then detected by western blotting using indicated antibodies. (*B*) Western blot analysis demonstrated that rapamycin, although less effective at inhibiting the growth of U87-EGFRvIII-PTEN cells, more completely inhibited S6K and S6 phorphorylation than did AICAR. (*C*) Reconstitution of PTEN desensitized U87-EGFRvIII glioblastoma cells to rapamycin, but not AICAR. Controls cells were treated by ethanol (1:1,000).

that the anti-growth properties of AICAR are not fully mediated through inhibition of mTORC1 signaling, but rather by effects on distinct AMPK targets.

AMPK Activation Mediates Its Growth Inhibition of Glioblastoma Cells Through Inhibition of Lipogenesis. AMPK is known to phosphorylate and negatively regulate Acetyl-CoA Carboxylase (ACC) and 3-hydroxy-3-methylglutaryl-CoA (HMG-CoA) reductase (Fig. 4*A*) pivotal enzymes in fatty acid and cholesterol synthesis, respectively (22, 23). Therefore, we asked whether AICAR's anti-growth effects were mediated, at least in part, through inhibition of lipogenesis. Thin layer chromatographic analysis of total lipid content demonstrated increased intracellular fatty acids in EGFRvIII-expressing glioblastoma cells relative to parental counterparts, which was fully abrogated by AICAR treatment (Fig. 4*B*). To determine whether AICAR's anti-growth effects were mediated through inhibition of lipogenesis, we asked whether addition of mevalonate and palmitate, the products of HMG-CoA reductase and fatty acid synthase (FAS), the enzyme catalyzing the downstream step of de novo fatty acid synthesis initiated by ACC, could rescue AICAR-mediated growth inhibition. As shown in Fig. 4*C*, addition of the 2 metabolites largely blocked the anti-growth effects of AICAR in U87-EGFR and U87-EGFRvIII expressing cells. These results suggested that the anti-proliferative effect of AICAR was mediated in a large part through inhibition of cholesterol and fatty acid synthesis. Therefore, we determined whether direct inhibition of cholesterol and fatty acid synthesis could also block glioblastoma growth by examining a panel of glioma cell lines expressing either relatively low levels of phosphorylated EGFR (U87, U373, U138, and LN229) or relatively high levels of phospho-EGFR (U87-EGFR, U87-EGFRvIII, and T98). Treatment with the HMG-CoA reductase inhibitor atorvastatin and the ACC inhibitor TOFA in combination, significantly inhibited tumor-cell proliferation in EGFR-activated glioblastoma cells with relatively minimal effects on non-EGFR activated cell lines (Fig. 4*D* and Figs. S4 and S5). Moreover, this inhibitory effect was largely

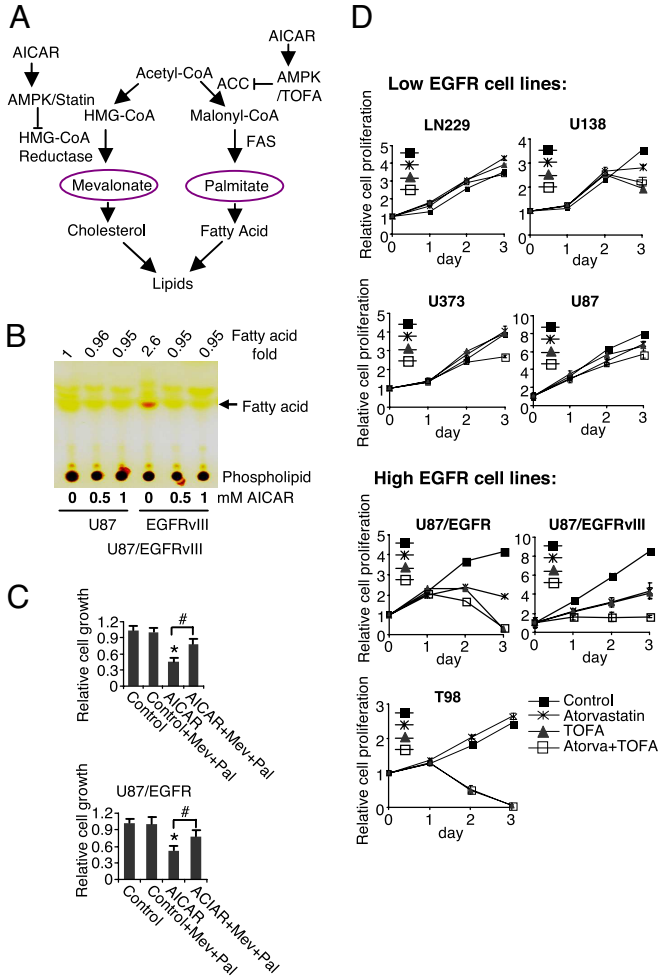

Fig. 4. The anti-proliferative effect of AMPK activation is mediated by inhibition of lipogenesis. (*A*) Schema showing how AICAR can potentially regulate lipogenesis. (*B*) Thin layer chromatography of total cellular lipids from serum starved cells showed increased intracellular fatty acids in EGFRvIII expressing cells, which was inhibited by AICAR treatment for 24 h. (*C*) Addition of mevalonate and palmitate rescued AICAR-mediated growth inhibition. U87-EGFRvIII and U87-EGFR cells were plated, 24 h later they were treated with AICAR (0.5 mM) alone or in combination with mevalonate and/or palmitate (100 μM). Cells were treated for 3 days and relative cell growth was determined by the WST assay (Chemicon). *, $P < 0.001$ compared with control; # $P < 0.01$. (*D*) Inhibition of HMG-CoA reductase (atorvastatin 1 μM) and acetyl-CoA carboxylase (ACC) (TOFA 10 μg/mL) preferentially blocked the growth of EGFR-activated glioblastoma cells. Control cells were treated with DMSO (1:1,000).

rescued by addition of mevalonate and palmitate (Fig. S6). Taken together these results indicate that AICAR's anti-growth effects were largely mediated through inhibition of cholesterol and fatty acid synthesis.

AICAR Blocks the Growth of EGFRvIII-expressing Glioblastomas in Vivo. To determine whether AICAR inhibits the growth of glioblastomas in vivo and to assess whether there is enhanced efficacy against EGFR-activated tumors, we implanted U87 or U87-EGFRvIII expressing tumor cells s.c. in immunodeficient SCID/Beige mice. Consistent with our in vitro findings, AICAR treatment promoted AMPK Thr-172 phosphorylation in both U87 and U87-EGFRvIII xenografts (Fig. 5*A*) and significantly inhibited the growth of EGFRvIII-containing tumors (40% inhibition relative to control, $P < 0.01$), whereas no growth inhibition was detected in U87 glioblastoma tumors lacking EGFRvIII (Fig. 5*B*). The effect

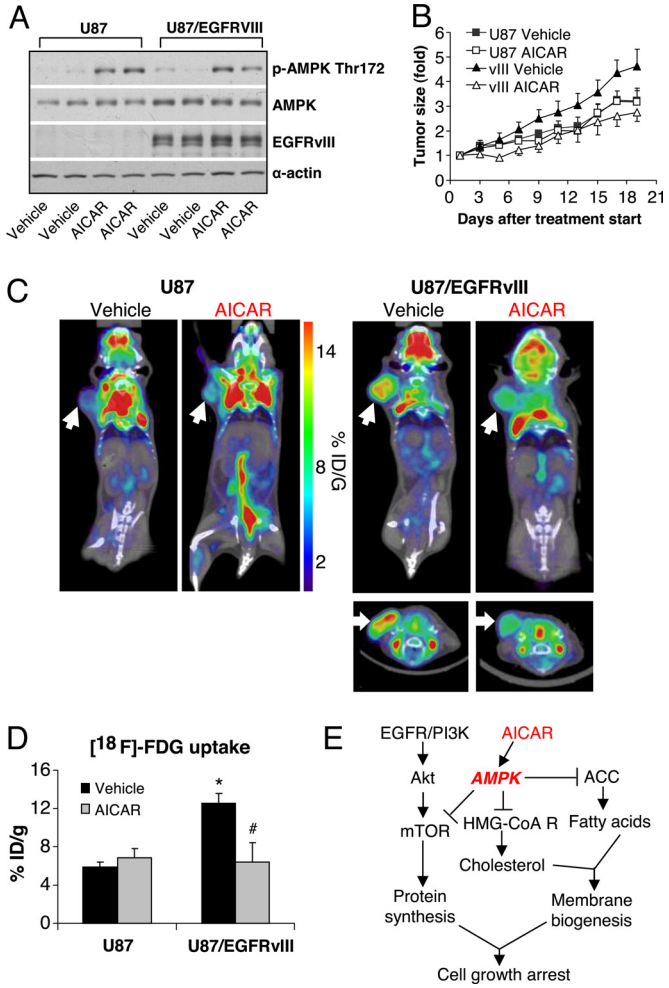

Fig. 5. AICAR blocks the growth of EGFRvIII expressing glioblastoma in vivo. (*A*) Western blot analysis of tumor xenograft lysates treated with AICAR (400 mg/kg) I.P. treatment for 3 days, or control (PBS only I.P. treatment), demonstrated AMPK Thr-172 phosphorylation in AICAR treated xenografts, but not control treated tumors. (*B*) AICAR significantly inhibited the growth of U87-EGFRvIII, but not U87 xenograft tumors, up to 21 days after initiation of treatment. Control mice were treated by PBS. (*C* and *D*) ^{18}F-FDG microPET/CT imaging demonstrated that EGFRvIII expressing tumors have higher baseline (day 3) uptake of ^{18}F-FDG relative to U87 cells; AICAR treatment (400 mg/kg for 3 days) greatly inhibited the ^{18}F-FDG uptake by EGFRvIII expressing tumors ($P < 0.001$); no such inhibition was detected in non-EGFRvIII expressing U87 tumors. *, $P < 0.001$ compared with U87 tumor vehicle (PBS) treatment; # $P < 0.01$ compared with U87/EGFRvIII tumor vehicle (PBS) treatment. (*E*) Schema showing the EGFR/PI3K/Akt/mTOR signaling pathway and the potential mechanism of AICAR-mediated growth inhibition.

was cytostatic, as no increase in TUNEL immunostaining was detected (Fig. S7).

Cancer cells undergo a marked shift toward aerobic glycolysis ("the Warburg effect") (24, 25) with coordinate redirecting of glycolytic intermediates from energy production toward anabolic processes, including fatty acid synthesis for generation of new membranes (26, 27). To determine whether AICAR treatment inhibited glucose metabolism, after 3 days of treatment, before the significant differences in tumor volumes, mice were imaged by microPET/CT to assess ^{18}F-2-deoxyglucose (^{18}F-FDG) uptake. EGFRvIII expression led to a highly significant increase in ^{18}F-FDG uptake at baseline, and AICAR treatment significantly inhibited ^{18}F-FDG uptake of U87-EGFRvIII expressing tumors in vivo (57% inhibition; $P < 0.01$) (Fig. 5*C* and *D*). In contrast, no such inhibition of glucose uptake was detected in the non-EGFRvIII expressing parental tumors with AICAR treatment (Fig. 5 *C* and *D*). These results raise the possibility that the efficacy of the AMPK agonist could potentially be non-invasively measured in patients using ^{18}F-FDG microPET to help determine dosing and therapeutic efficacy.

Discussion

In summary, we demonstrate that the AMPK agonist AICAR can preferentially inhibit the growth and lipogenesis of EGFR-activated glioblastoma cells. AICAR has been postulated to mediate its anti-growth effects primarily through mTOR inhibition (14, 28). Thus, the demonstration that its effects were mediated primarily through inhibition of lipogenesis was quite unexpected. We show that EGFRvIII, in addition to activating mTOR/S6K/S6 signaling, enhances lipogenesis, potentially conferring enhanced sensitivity to AICAR. Cancer cells undergo a marked shift toward aerobic glycolysis ("the Warburg effect") with coordinate redirecting of glycolytic intermediates from energy production toward anabolic processes (27). EGFRvIII enhanced ^{18}F-FDG uptake in glioblastoma in vivo, and AICAR treatment coordinately blocked glucose uptake and lipogenesis (Fig. 5*C* and *D*), suggesting that these processes were co-regulated. These results suggest that AICAR may disrupt a critical link by which persistent EGFR signaling promotes tumor growth through coordinate regulation of protein synthesis and lipogenesis (Fig. 5*E*). These results suggest a potential therapeutic strategy for EGFR-activated cancers.

In this paper, we demonstrate a link between EGFR signaling and sensitivity to the AMPK agonist AICAR. However, these studies do not address whether this is mediated by direct interactions between EGFR signaling and AMPK. Recent work demonstrates a molecular link by which RAF-MEK-ERK signaling in B-RAF mutant melanomas promotes tumor cell growth through phosphorylation of LKB1 and subsequent suppression of AMPK phosphorylation (29). This study raises the possibility that other common cancer mutants that strongly activate ERK and p90Rsk could also potentially inhibit AMPK phosphorylation to promote tumor cell growth. Future studies will be needed to determine whether persistently mutant EGFR signaling, or other activated receptor tyrosine kinases, can inhibit AMPK phoshorylation, and whether it is mediated through RAF-MEK-ERK dependent phosphorylation of LKB1. In addition, other receptor tyrosine kinase (RTK) commonly expressed in glioblastoma may also activate mTORC1. It will be important to determine whether those other RTK's could potentially regulate LKB1-AMPK signaling and determine response to AICAR.

Our finding that AICAR was more effective than rapamycin, despite only partial inhibition of mTORC1 signaling, does not limit the importance of mTORC1 as a therapeutic target. mTORC1 integrates input from multiple signaling pathways, such as growth factor signaling through class I PI3K and potentially through PKC alpha (6), and amino acid sensing through a class 3 PI3K (VPS34) (30–32). Elevated mTORC1 signaling is common in glioblastoma, particularly in patients with EGFR-activated tumors (5, 6), and it is associated with shorter patient survival (33). mTORC1 signaling also appears to play a key role in gliomagenesis and in response to targeted therapies. S6K1 activation, downstream of mTORC1, has recently been shown to be a critical step for glial transformation (4), and a critical regulator of response to EGFR kinase inhibitors (6). Thus, successful inhibition of mTORC1 may be important for treating glioblastoma patients. Consistent with the recent finding of Fan and colleagues, our study demonstrates a link between EGFR and mTORC1 that may be independent of Akt (6). We have previously shown that the failure of rapamycin in patients may be mediated both by insufficient target inhibition and by feedback activation of Akt (10). To our surprise, the enhanced efficacy of AICAR relative to rapamycin was not mediated by mTORC1 inhibition. AICAR only partially inhibited mTORC1 (Fig. 3*A*), which may explain the lack of feedback Akt activation. Further, we

observed additive benefit against EGFR-activated cell lines when AICAR and rapamycin were combined (Fig. S3). Our study clearly implicates AMPK as a potentially important molecular target in glioblastoma, particularly in EGFR-activated tumors. The penetration of AICAR, and other AMPK agonists across the blood brain barrier into gliomas, in which the blood brain barrier is partially abrogated, is not well understood. Future studies will be needed to identify AMPK activators that can readily access intracranial tumors. In addition, it will be important to determine whether there is benefit in combining mTORC1 inhibitors with AMPK agonists, particularly now with the development of ATP-competitive mTOR inhibitors that block both mTORC1 and mTORC2 and that inhibit rapamycin-resistant signaling through mTORC1 (34).

Materials and Methods

Cell Lines. Glioma cell lines T98, LN229, U373, U138, and U87, were purchased from American Tissue Culture Collection (ATCC). EGFRvIII expressing U87 cells were obtained as a kind gift from Dr. Webster Cavenee. U87/EGFR cells were constructed as previously described (16, 17), A431 skin cancer cells were obtained from ATCC. All of these cell lines were cultured in DMEM (Cellgro) supplemented with 10% FBS (Omega Scientific) in a humidified atmosphere of 5% CO_2, 95% air at 37 °C. H1975 Non-small cell lung carcinoma cell line (NSCLC) were obtained from ATCC and cultured in RPM 1640 with 10% FBS.

Antibodies and Reagents. The following antibodies: *p*-AMPK Thr-172, AMPK, *p*-ACC Ser-79, ACC, FAS, *p*-Akt Thr-308, *p*-Akt Ser-473, Akt, *p*-S6k Thr-389, S6k, *p*-S6 Ser-235/236, *p*-S6 Ser-240/244, S6, PTEN, *p*-GSK3β, and GSK3β (Cell Signaling); α-actin (Sigma); EGFR (Upstate) were used. Ad-AMPK-CA was used to overexpress a constitutively active AMPK mutant (35), and the parental adenoviral vector (Ad-null) was referred to as null, when used as a control. AMPKα1/α2 siRNA, a mixture of AMPK α1 and α2 isoforms siRNA was purchased from Santa Cruz. Compound C was purchased from Calbiochem.

Cell Proliferation Assay. Tumor cells were seeded in 96-well plates for 24 h and treated with inhibitors for 3 days. Relative proliferation was assessed using the WST Cell Proliferation Assay Kit (Chemicon). In addition, trypan blue exclusion method was used to count viable cells.

Western Blotting. Immunoblot analyses were performed as previously described (12).

Colony Formation Assay. Cells were seeded at a density of 500 cells per 60-mm dish. 24 h later, medium was changed and drugs were added, as indicated. Medium replenished with drugs was changed every 3 days. Three weeks after initial treatment, cultures were fixed with 4% formaldehyde (Sigma) in PBS and stained with a 0.5% crystal violet solution (Sigma) in 25% methanol. Colonies of more than 50 cells were counted (36).

Thin Layer Chromatography for Lipids. Cellular total lipid extract was obtained by scraping cells from the 10-cm culture dish into 2 mL PBS containing protease inhibitor and 1 mM PMSF and adding 4 mL chloroform/methanol (2:1, vol/vol) with 0.01% butylated hydroxytoluene (Sigma). The solution was vortexed and centrifuged at 1,500 $\times$ *g* for 5 min. The organic phase was collected and 2.5 mL chloroform was added to the residual aqueous phase which was vortexed and centrifuged at 1,500 $\times$ *g* for 5 min. The organic phase was pooled with the previous extraction. Thin layer chromatography (TLC) was performed by spotting of the cellular total lipid extract to a 5 $\times$ 10 cm silica gel aluminum sheet (EMD Chemicals) and developed with hexane/diethyl ether/acetic acid (80:20:2, vol/vol/v). Lipids were visualized with iodine vapor and imaged using a desktop scanner (37).

Xenograft Model. Isogenic human U87 malignant glioma cells (U87, U87/EGFRvIII) were implanted into immunodeficient SCID/Beige mice for s.c. (s.c.) xenograft studies. SCID/Beige mice were bred and kept under defined-flora pathogen-free conditions at the AALAC-approved Animal Facility of the Division of Experimental Radiation Oncology, UCLA. For s.c. implantation, exponentially growing tumor cells in culture were trypsinized, enumerated via Trypan Blue exclusion, and resuspended at 1 $\times$ 10^6 cells/mL in a solution of dPBS and Matrigel (BD Biosciences). Tumor growth was monitored with calipers by measuring the perpendicular diameters of each s.c. tumor. For imaging and AICAR treatment studies tumors were implanted s.c. on the left shoulder (n = 20). Mice bearing xenografts of U87 or U87/EGFRvIII cells underwent ^{18}F-2-deoxyglucose (FDG) positron emission tomography (microPET)/computed tomography (CT) scans when the tumor size had reached 100 cm^2. Following the microPET/CT study, groups of 5 mice were treated with AICAR (400 mg/kg, Toronto Research Chemicals) daily (36), 3 days later, a follow-up microPET/CT study was done using the same image acquisition variables (38). Mice were euthanized if tumors reached 14 mm in maximum diameter, or animals showed signs of illness. All experiments were conducted after approval by the Chancellor's Animal Research Committee of UCLA.

MicroPET/CT Imaging. Mice were kept warm, under gas anesthesia (2% isoflourane) and injected with ^{18}F-FDG (i.p). A 1-h interval for uptake was allowed between probe administration and microPET/CT scanning. For ^{18}F-FDG scans, animals were fasted before imaging (6 h) and blood glucose levels were measured to ensure similar experimental conditions. Data were acquired using a Siemens Preclinical Solutions microPET Focus 220 and a MicroCAT II CT instrument. MicroPET data were acquired for 10 min and was reconstructed using statistical maximum a posteriori probability algorithms (MAP) into multiple frames (39). The spatial resolution of microPET is approximately 1.5-mm, 0.4-mm voxel size. CT images are at low dose 400-μm resolution acquisition, with 200-μm voxel size. MicroPET and microCT images were co-registered using a previously described method (40). Three-dimensional regions of interest (ROI) were drawn using AMIDE software (Andreas Loening) (41). Color scale is proportional to tissue concentration with red being the highest and lower values in yellow, green, and blue.

Statistical Analysis. Results are shown as mean $\pm$ SEM, which were performed using 2-tailed t test as well as by ANOVA as appropriate. $P < 0.05$ was considered as statistically significant.

ACKNOWLEDGMENTS. We thank Dr. George Thomas for his careful reading of the manuscript and helpful comments. This work was supported by National Institute for Neurological Disorders and Stroke Grant NS050151, National Cancer Institute Grants CA119347 and CA108633, the Brain Tumor Funders' Collaborative, and Accelerate Brain Cancer Cure (to P.S.M.) and the Harry Allgauer Foundation through The Doris R. Ullman Fund for Brain Tumor Research Technologies, the Henry E. Singleton Brain Tumor Program, and generous donations from the Ziering Family Foundation in memory of Sigi Ziering and Timothy and Mary Haneman.

1. Yap TA, et al. (2008) Targeting the PI3K-AKT-mTOR pathway: Progress, pitfalls, and promises. *Curr Opin Pharmacol* 8:393–412.
2. Guertin DA, Sabatini DM (2007) Defining the role of mTOR in cancer. *Cancer Cell* 12:9–22.
3. Shaw RJ, Cantley LC (2006) Ras, PI(3)K and mTOR signaling controls tumor cell growth. *Nature* 441:424–430.
4. Nakamura JL, Garcia E, Pieper RO (2008) S6K1 plays a key role in glial transformation. *Cancer Res* 68:6516–6523.
5. Choe G, et al. (2003) Analysis of the phosphatidylinositol 3′-kinase signaling pathway in glioblastoma patients in vivo. *Cancer Res* 63:2742–2746.
6. Fan QW, et al. (2009) EGFR signals to mTOR through PKC and independently of Akt in glioma. *Sci Signal* 2:ra4.
7. Kreisl TN, et al. (2009) A pilot study of everolimus and gefitinib in the treatment of recurrent glioblastoma (GBM). *J Neurooncol* 92:99–105.
8. Doherty L, et al. (2006) Pilot study of the combination of EGFR and mTOR inhibitors in recurrent malignant gliomas. *Neurology* 67:156–158.
9. Chang SM, et al. (2005) Phase II study of CCI-779 in patients with recurrent glioblastoma multiforme. *Invest New Drugs* 23:357–361.
10. Cloughesy TF, et al. (2008) Antitumor activity of rapamycin in a Phase I trial for patients with recurrent PTEN-deficient glioblastoma. *PLoS Med* 5:e8.
11. Carracedo A, et al. (2008) Inhibition of mTORC1 leads to MAPK pathway activation through a PI3K-dependent feedback loop in human cancer. *J Clin Invest* 118:3065–3074.
12. Guo D, Chien S, Shyy JY (2007) Regulation of endothelial cell cycle by laminar versus oscillatory flow: Distinct modes of interactions of AMP-activated protein kinase and Akt pathways. *Circ Res* 100:564–571.
13. Inoki K, Zhu T, Guan KL (2003) TSC2 mediates cellular energy response to control cell growth and survival. *Cell* 115:577–590.
14. Gwinn DM, et al. (2008) AMPK phosphorylation of raptor mediates a metabolic checkpoint. *Mol Cell* 30:214–226.
15. Zhang H, et al. (2007) PDGFRs are critical for PI3K/Akt activation and negatively regulated by mTOR. *J Clin Invest* 117:730–738.
16. Mellinghoff IK, et al. (2005) Molecular determinants of the response of glioblastomas to EGFR kinase inhibitors. *N Engl J Med* 353:2012–2024.
17. Wang MY, et al. (2006) Mammalian target of rapamycin inhibition promotes response to epidermal growth factor receptor kinase inhibitors in PTEN-deficient and PTEN-intact glioblastoma cells. *Cancer Res* 66:7864–7869.

18. Shtiegman K, et al. (2007) Defective ubiquitinylation of EGFR mutants of lung cancer confers prolonged signaling. *Oncogene* 26:6968–6978.
19. Zhou G, et al. (2001) Role of AMP-activated protein kinase in mechanism of metformin action. *J Clin Invest* 108:1167–1174.
20. Towler MC, Hardie DG (2007) AMP-activated protein kinase in metabolic control and insulin signaling. *Circ Res* 100:328–341.
21. Neshat MS, et al. (2001) Enhanced sensitivity of PTEN-deficient tumors to inhibition of FRAP/mTOR. *Proc Natl Acad Sci USA* 98:10314–10319.
22. Carling D, et al. (1994) Mammalian AMP-activated protein kinase is homologous to yeast and plant protein kinases involved in the regulation of carbon metabolism. *J Biol Chem* 269:11442–11448.
23. Sullivan JE, Carey F, Carling D, Beri RK (1994) Characterisation of 5′-AMP-activated protein kinase in human liver using specific peptide substrates and the effects of 5′-AMP analogues on enzyme activity. *Biochem Biophys Res Commun* 200:1551–1556.
24. Warburg O (1956) On the origin of cancer cells. *Science* 123:309–314.
25. Warburg O (1956) On respiratory impairment in cancer cells. *Science* 124:269–270.
26. Christofk HR, et al. (2008) The M2 splice isoform of pyruvate kinase is important for cancer metabolism and tumour growth. *Nature* 452:230–233.
27. DeBerardinis RJ, Lum JJ, Hatzivassiliou G, Thompson CB (2008) The biology of cancer: metabolic reprogramming fuels cell growth and proliferation. *Cell Metab* 7:11–20.
28. Gleason CE, Lu D, Witters LA, Newgard CB, Birnbaum MJ (2007) The role of AMPK and mTOR in nutrient sensing in pancreatic beta-cells. *J Biol Chem* 282:10341–10351.
29. Zheng B, et al. (2009) Oncogenic B-RAF negatively regulates the tumor suppressor LKB1 to promote melanoma cell proliferation. *Mol Cell* 33:237–247.
30. Nobukuni T, et al. (2005) Amino acids mediate mTOR/raptor signaling through activation of class 3 phosphatidylinositol 3OH-kinase. *Proc Natl Acad Sci USA* 102:14238–14243.
31. Gulati P, et al. (2008) Amino acids activate mTOR complex 1 via Ca2+/CaM signaling to hVps34. *Cell Metab* 7:456–465.
32. Carracedo A, Baselga J, Pandolfi PP (2008) Deconstructing feedback-signaling networks to improve anticancer therapy with mTORC1 inhibitors. *Cell Cycle* 7:3805–3809.
33. Chakravarti A, et al. (2004) The prognostic significance of phosphatidylinositol 3-kinase pathway activation in human gliomas. *J Clin Oncol* 22:1926–1933.
34. Thoreen CC, et al. (2009) An ATP-competitive mammalian target of rapamycin inhibitor reveals rapamycin-resistant functions of mTORC1. *J Biol Chem* 284:8023–8032.
35. Foretz M, et al. (2005) Short-term overexpression of a constitutively active form of AMP-activated protein kinase in the liver leads to mild hypoglycemia and fatty liver. *Diabetes* 54:1331–1339.
36. Swinnen JV, et al. (2005) Mimicry of a cellular low energy status blocks tumor cell anabolism and suppresses the malignant phenotype. *Cancer Res* 65:2441–2448.
37. Watson AD (2006) Thematic review series: systems biology approaches to metabolic and cardiovascular disorders. Lipidomics: A global approach to lipid analysis in biological systems. *J Lipid Res* 47:2101–2111.
38. Wei LH, et al. (2008) Changes in tumor metabolism as readout for Mammalian target of rapamycin kinase inhibition by rapamycin in glioblastoma. *Clin* Cancer Res 14:3416–3426.
39. Qi J, Leahy RM, Cherry SR, Chatziioannou A, Farquhar TH (1998) High-resolution 3D Bayesian image reconstruction using the microPET small-animal scanner. *Phys Med Biol* 43:1001–1013.
40. Chow PL, Stout DB, Komisopoulou E, Chatziioannou AF (2006) A method of image registration for small animal, multi-modality imaging. *Phys Med Biol* 51:379–390.
41. Loening AM, Gambhir SS (2003) AMIDE: A free software tool for multimodality medical image analysis. *Mol Imaging* 2:131–137.